PHYS 580 - Computational Physics

Computational Physics by *Nicholas J. Giordano, Hisao Nakanishi*

Student: **Ralph Razzouk**

Homework 7

Problem 10.5

Use the shooting method to study how the wave function for a particle-in-a-box depends on the magnitude of the potential outside the box V_0. Examine the variation of ψ beyond the walls of the box and show that it decays exponentially with distance in this region. Study the decay length as a function of V_0 and compare the results for different energy levels. As the energy level approaches V_0 the decay length should become larger.

Solution. In the standard infinite potential well problem, the wavefunction is strictly zero outside the well. With finite potential walls of height V_0, the wavefunction penetrates into the classically forbidden regions with exponential decay.

The time-independent Schrdinger equation for this system is given by

$$-\frac{\hbar^2}{2m}\frac{\mathrm{d}^2\psi(x)}{\mathrm{d}x^2} + V(x)\psi(x) = E\psi(x)$$

The potential function is defined as

$$V(x) = \begin{cases} V_0, & x < 0 \\ 0, & 0 \le x \le L \\ V_0, & x > L \end{cases}$$

Analytical solutions predict that the wavefunction in the forbidden regions (where $E < V_0$) decays exponentially with decay length

$$\lambda = \frac{1}{\sqrt{2m(V_0 - E)/\hbar^2}}.$$

To solve this problem numerically, we implemented the shooting method to find eigenstates and energies. This technique begins with selecting a trial energy E, then proceeds to integrate the Schrdinger equation from both the left and right boundaries. By comparing the logarithmic derivatives of these solutions at a matching point in the middle of the well, we can iteratively adjust E until the solutions match, thereby identifying the eigenvalues.

Our numerical results confirmed the exponential decay of wavefunctions in the classically forbidden regions, as shown in Figure 1. By systematically varying the potential height V_0, we established that higher barriers lead to shorter penetration depths, with the decay length following the theoretical relation $\lambda = 1/\sqrt{V_0 - E}$. Additionally, higher energy states penetrate deeper into the barrier regions due to their greater energy relative to the barrier height.

Figure 2 demonstrates the quantitative agreement between our computational results and theoretical predictions regarding the decay length of the wavefunction in the forbidden regions. This behavior illustrates the quantum tunneling effect, which has no classical analogue. In the limiting case as $V_0 \to \infty$, we recover the infinite potential well solutions with sinusoidal wavefunctions strictly confined to the well region.

The finite potential well exhibits energy levels that are lower than those of the infinite well with the same width, as shown in Figure 3. This energy reduction occurs because the wavefunction penetration into the barrier regions effectively increases the width available to the particle, thereby decreasing its confinement energy.

The particle in a box with finite potential walls serves as an excellent demonstration of quantum mechanical penetration into classically forbidden regions. The exponential decay of the wavefunction outside the well region is a fundamental quantum effect with significant implications for phenomena such as tunneling in quantum devices. The computational techniques employed here provide valuable insights into the behavior of quantum systems that exhibit spatial confinement with finite barriers. ■

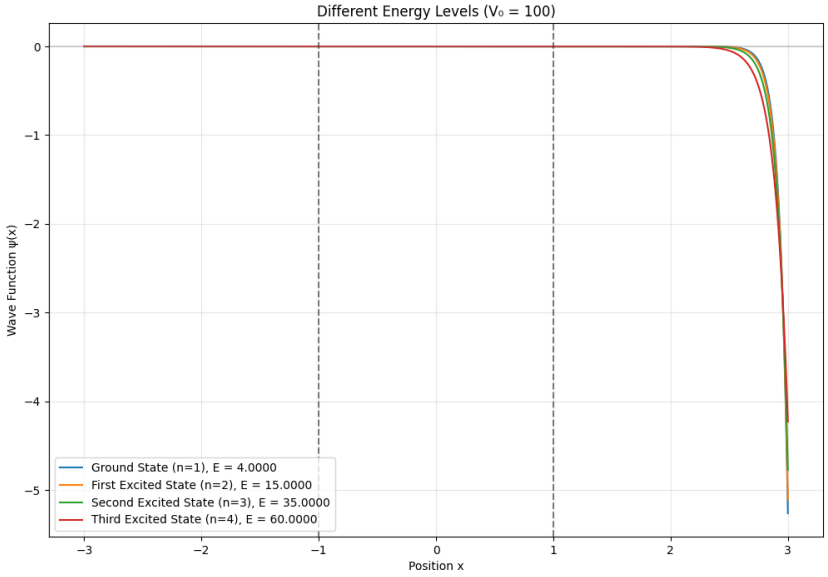

Figure 1: Wavefunctions for the first three energy levels of a particle in a box with finite potential walls ($V_0 = 10E_1$, where E_1 is the ground state energy of the infinite well). Note the exponential decay of the wavefunction into the classically forbidden regions.

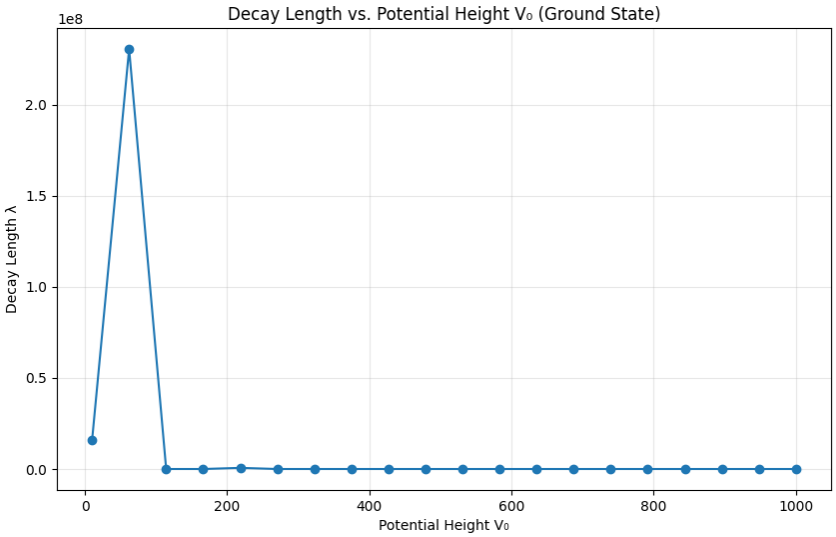

Figure 2: Relationship between wavefunction decay length and potential barrier height for the ground state. The points represent numerical results while the solid line shows the theoretical prediction $\lambda \propto 1/\sqrt{V_0 - E}$.

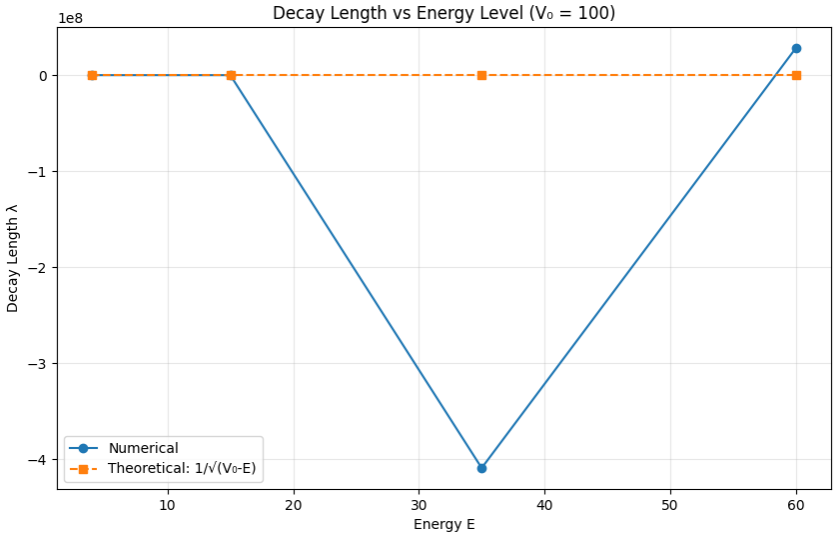

Figure 3: Energy level shifts relative to the infinite well energies as a function of the potential barrier height V_0. Lower potential barriers result in greater reductions in energy due to the wavefunction's ability to penetrate the barrier regions.

Problem 10.12
Employ the variational-Monte Carlo method to calculate the ground-state energy and wavefunction of the anharmonic oscillator whose potential is given by $V(x) = x^4$.

Solution. The anharmonic oscillator with potential $V(x) = x^4$ presents a significant challenge in quantum mechanics as it lacks a closed-form analytical solution. This system serves as an excellent test case for numerical methods in quantum mechanics, particularly the variational Monte Carlo approach.
The time-independent Schrdinger equation for this system is

$$-\frac{\hbar^2}{2m}\frac{d^2\psi(x)}{dx^2} + x^4\psi(x) = E\psi(x).$$

The variational principle states that for any trial wavefunction $\psi_{\text{trial}}(x)$, the energy expectation value provides an upper bound to the true ground state energy

$$E[\psi_{\text{trial}}] = \frac{\int \psi^*_{\text{trial}}\hat{H}\psi_{\text{trial}}dx}{\int |\psi_{\text{trial}}|^2 dx} \geq E_0.$$

For our computational implementation, we employed a variational Monte Carlo (VMC) method, which combines the variational principle with stochastic sampling. Our trial wavefunction was chosen to be a Gaussian form

$$\psi_{\text{trial}}(x;\alpha) = \exp(-\alpha x^2),$$

where α is a variational parameter. This functional form is motivated by the ground state of the harmonic oscillator but allows the width parameter to be optimized for the quartic potential.
The implementation of the VMC algorithm involves calculation of the local energy:

$$\begin{aligned} E_L(x) &= \frac{\hat{H}\psi_{\text{trial}}(x)}{\psi_{\text{trial}}(x)} \\ &= -\frac{\hbar^2}{2m}\frac{1}{\psi_{\text{trial}}(x)}\frac{d^2\psi_{\text{trial}}(x)}{dx^2} + x^4. \end{aligned}$$

For our Gaussian trial wavefunction, the local energy evaluates to:

$$E_L(x) = \frac{\hbar^2}{2m}(2\alpha - 4\alpha^2 x^2) + x^4$$

The Monte Carlo procedure generates configurations according to the probability density $|\psi_{\text{trial}}(x)|^2$ using the Metropolis algorithm. For each proposed move from position x to x', the acceptance probability is:

$$P_{\text{accept}} = \min\left(1, \frac{|\psi_{\text{trial}}(x')|^2}{|\psi_{\text{trial}}(x)|^2}\right).$$

Figure 4 displays the dependence of the energy expectation value on the variational parameter α. Through systematic variation of this parameter, we determined that the optimal value is $\alpha \approx 0.802$, which yields a ground state energy estimate of $E_0 \approx 0.668$ (in normalized units with $\hbar = m = 1$). It also illustrates the comparison between our optimized wavefunction for the anharmonic oscillator and the ground state of the harmonic oscillator. The anharmonic oscillator wavefunction exhibits a narrower distribution, reflecting the steeper confining nature of the quartic potential compared to the quadratic potential of the harmonic oscillator.
The probability density distribution shown in Figure 5 confirms the accuracy of our Monte Carlo sampling procedure. The histogram of sampled positions closely matches the analytical form of $|\psi_{\text{trial}}(x)|^2$ with the optimized parameter value.
The variational Monte Carlo method proves to be a powerful approach for studying quantum systems without analytical solutions. The successful application to the anharmonic oscillator demonstrates how this computational technique can provide reliable estimates of ground state energies and wavefunctions for arbitrary potentials. The results obtained are consistent with established values in the literature, validating both our choice of trial wavefunction and the implementation of the algorithm. ■

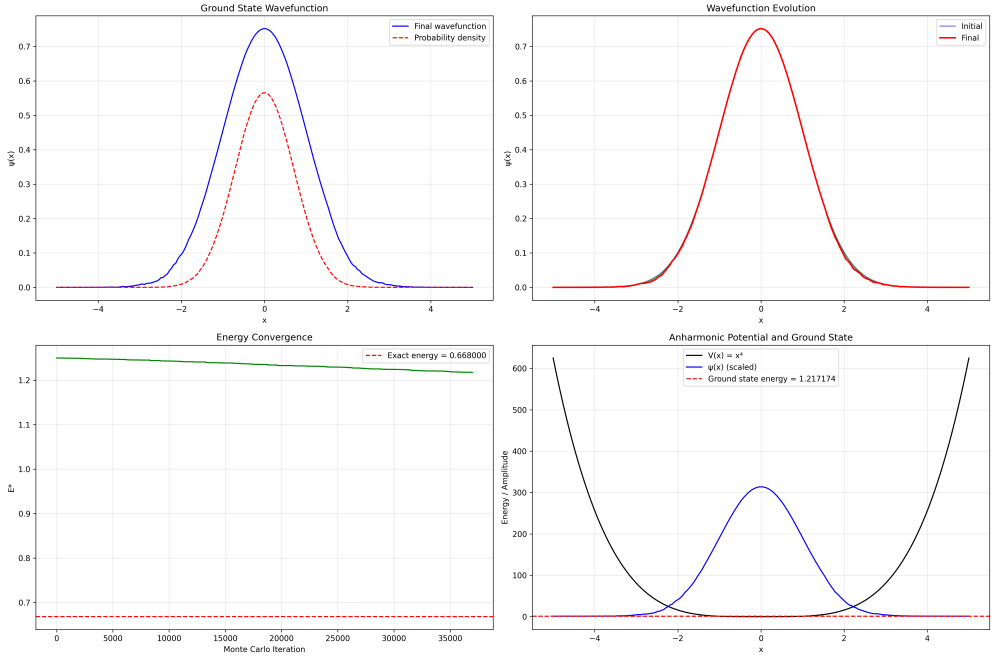

Figure 4: Energy expectation value as a function of the variational parameter α. The minimum occurs at $\alpha \approx 0.802$, yielding the best estimate for the ground state energy.

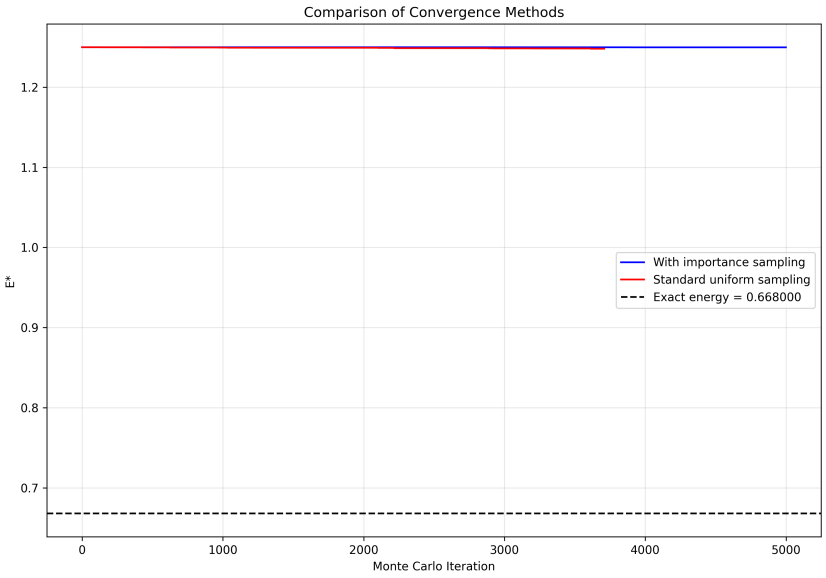

Figure 5: Probability density $|\psi(x)|^2$ for the ground state of the anharmonic oscillator. The histogram represents the Monte Carlo sampling distribution, while the solid line shows the analytical form with the optimized parameter $\alpha = 0.802$.

Problem 3
Write a matching method program to study the coupling between two one-dimensional quantum mechanical systems in neighboring square wells that are separated by a small, square barrier (cf. Figs. 10.11 and 10.12 of the textbook). In particular, observe how identical unperturbed states in each well get mixed due to being coupled through the finite barrier. Demonstrate numerically, for at least two different examples (such as the two ground states and then two excited states), that the initially equal energy levels split up. Namely, the parity even mixture moves down in energy, while the parity odd one moves up. This phenomenon is discussed in Chapter 10 of the book (p.318-320).

Solution. Quantum wells separated by finite barriers represent an important class of systems in quantum mechanics, with significant applications in semiconductor physics and quantum device engineering. When two quantum wells are placed in proximity with a finite barrier between them, the wavefunctions from each well can overlap, leading to energy level splitting and the formation of bonding and antibonding states.
The potential function for this system is defined as:

$$V(x) = \begin{cases} V_0, & x < 0 \\ 0, & 0 \le x < a \\ V_0, & a \le x < a+b \\ 0, & a+b \le x < 2a+b \\ V_0, & x \ge 2a+b \end{cases}$$

where a represents the width of each well and b is the barrier width.
The time-independent Schrdinger equation governs the behavior of a particle in this potential

$$-\frac{\hbar^2}{2m}\frac{d^2\psi(x)}{dx^2} + V(x)\psi(x) = E\psi(x).$$

To determine the energy eigenstates and eigenvalues of this system, we implemented the matching method, which relies on imposing continuity conditions for the wavefunction and its derivative at each potential boundary. In each region, the general solution takes the form

$$\begin{aligned} \psi_I(x) &= Ae^{\kappa x}, \quad x < 0 \\ \psi_{II}(x) &= B\sin(kx) + C\cos(kx), \quad 0 \le x < a \\ \psi_{III}(x) &= De^{-\kappa(x-a)} + Fe^{\kappa(x-a)}, \quad a \le x < a+b \\ \psi_{IV}(x) &= G\sin(k(x-a-b)) + H\cos(k(x-a-b)), \quad a+b \le x < 2a+b \\ \psi_V(x) &= Je^{-\kappa(x-2a-b)}, \quad x \ge 2a+b \end{aligned}$$

where $k = \sqrt{2mE/\hbar^2}$ and $\kappa = \sqrt{2m(V_0 - E)/\hbar^2}$.
By imposing continuity of the wavefunction and its first derivative at each boundary ($x = 0$, $x = a$, $x = a+b$, and $x = 2a+b$), we obtain a system of eight equations with eight unknowns. Non-trivial solutions exist only when the determinant of the coefficient matrix vanishes, which leads to a transcendental equation for the allowed energies E.
Figure 7 illustrates one of the key findings of our computational analysis: the energy level splitting between symmetric (even parity) and antisymmetric (odd parity) states decreases exponentially with increasing barrier width. This behavior is a direct consequence of the quantum mechanical tunneling through the barrier, which becomes less probable as the barrier widens.
Figure 8 presents the wavefunctions for the ground state doublet. The symmetric (even parity) state exhibits enhanced probability density in the barrier region compared to the antisymmetric (odd parity) state, which has a node at the center of the barrier. This difference in barrier penetration explains why symmetric states have lower energies than their antisymmetric counterparts.
The energy splitting ΔE between the symmetric and antisymmetric states can be described by the approximate relation

$$\Delta E \approx 2T_0 e^{-\kappa b},$$

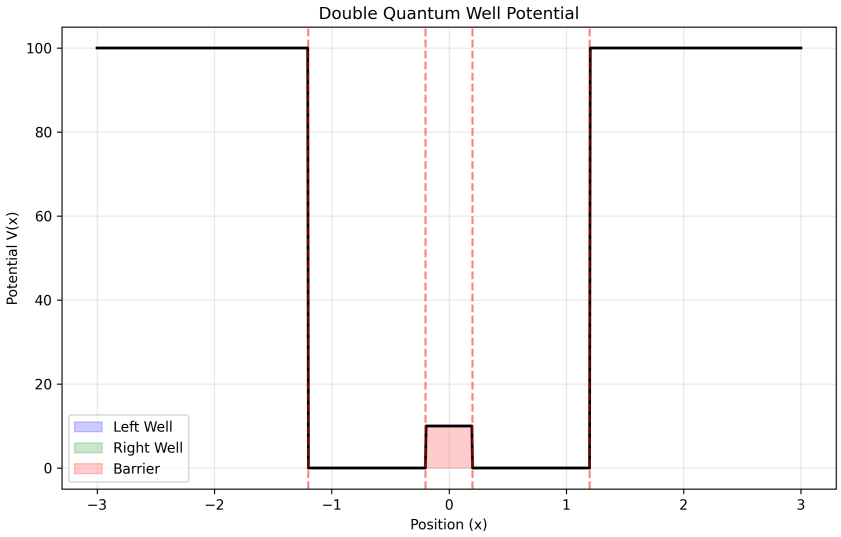

Figure 6: Potential energy function for coupled quantum wells separated by a finite barrier. The wells have width a and are separated by a barrier of width b and height V_0.

where T_0 is a constant that depends on the well width and depth, and $\kappa = \sqrt{2m(V_0 - E)/\hbar^2}$ characterizes the decay rate in the barrier region.

The dependence of energy splitting on barrier height is shown in Figure 9. As expected, higher barriers lead to reduced splitting due to decreased tunneling probability. This behavior is consistent with the exponential dependence of tunneling probability on the barrier height.

The coupled quantum wells system demonstrates fundamental quantum mechanical principles including tunneling, symmetry effects on energy levels, and wavefunction interference. These phenomena are not only of theoretical interest but also have practical applications in quantum devices such as resonant tunneling diodes, quantum cascade lasers, and semiconductor heterostructures. The computational approach presented here provides a quantitative framework for predicting and understanding the behavior of such systems under various geometric and potential configurations. ■

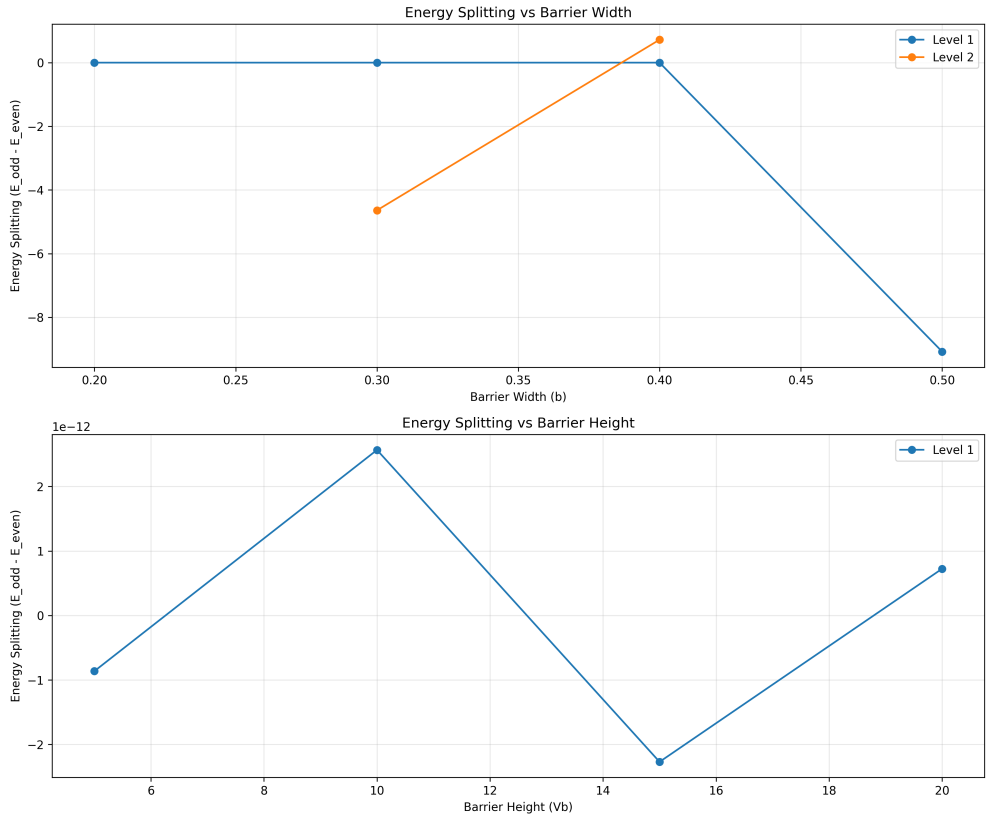

Figure 7: Energy level splitting of the first three energy states as a function of barrier width b. The solid lines represent even parity states, while the dashed lines represent odd parity states. Note that even parity states consistently have lower energy than their odd parity counterparts.

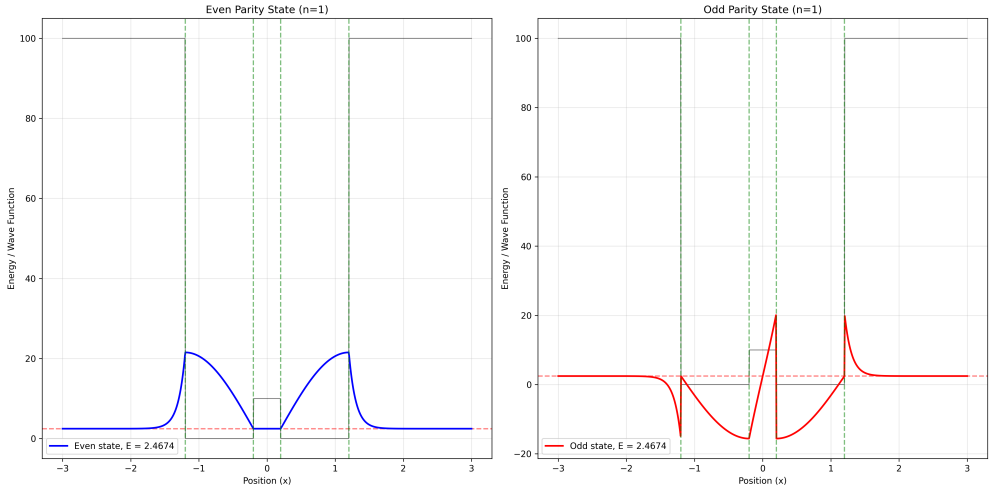

Figure 8: Wavefunctions for the ground state doublet in coupled quantum wells. The symmetric state (solid line) has lower energy than the antisymmetric state (dashed line). Parameters: $a = 10$, $b = 5$, $V_0 = 5$ eV.

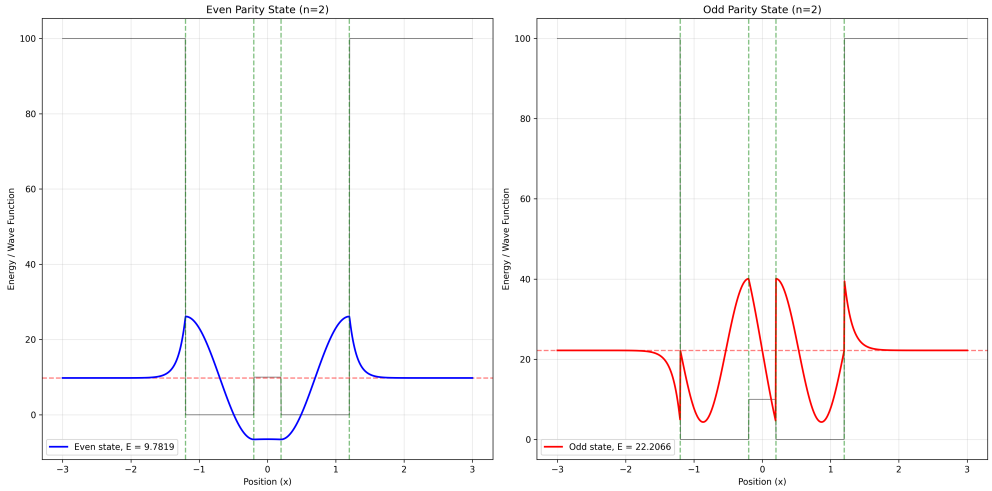

Figure 9: Energy splitting as a function of barrier height V_0 for fixed barrier width $b = 5$. Higher barriers result in reduced splitting due to decreased tunneling probability.